Conversion of agricultural residues into activated carbons for water purification: Application to arsenate removal

Jonatan Torres-Perez, Claire Gerente, Yves Andres

Conversion of agricultural residues into activated carbons for water purification: Application to arsenate removal

JONATAN TORRES-PEREZ[1,2], CLAIRE GERENTE[2] andYVES ANDRES[2]

[1]Centro Interamericano de Recursos del Agua, Facultad de Ingenieria, Universidad Autonoma del Estado de Mexico, Cerro de Coatepec, Ciudad Universitaria, Toluca, Estado de Mexico, Mexico
[2]LUNAM Université, Ecole des Mines de Nantes, CNRS, GEPEA, Nantes, France

The conversion of two agricultural wastes, sugar beet pulp and peanut hulls, into sustainable activated carbons is presented and their potential application for the treatment of arsenate solution is investigated. A direct and physical activation is selected as well as a simple chemical treatment of the adsorbents. The material properties, such as BET surface areas, porous volumes, elemental analysis, ash contents and pH_{PZC}, of these alternative carbonaceous porous materials are determined and compared with a commercial granular activated carbon. An adsorption study based on experimental kinetic and equilibrium data is conducted in a batch reactor and completed by the use of different models (intraparticle diffusion, pseudo–second-order, Langmuir and Freundlich) and by isotherms carried out in natural waters. It is thus demonstrated that sugar beet pulp and peanut hulls are good precursors to obtain activated carbons for arsenate removal.

Keywords: Activated carbon, adsorption, arsenate, iron impregnation, residue valorization, water treatment.

Introduction

Activated carbon (AC) is currently one of the most used adsorbents for water and air purification on an industrial scale. The production process is commonly divided in 2 steps: pyrolysis of the precursor (coal, coconut, wood, etc.) followed by its activation to create porosity. The first step is often conducted where the precursor is locally produced while the second occurs in another place from where the ACs are distributed all around the world.

In 2007, Ioannidou and Zabaniotou[1] published a review documenting more than 100 references about activated carbon production from agricultural residues on a laboratory scale. They concluded that steam or CO_2 activation is easier to handle, cleaner and cheaper than chemical activation. Moreover, if this treatment is conducted in a one-step process (direct activation), there is also an economic benefit. However, depending on the nature of the precursors, these ACs exhibit less satisfactory characteristics for further use as adsorbents or filters.[1] In terms of residue valorization, the main idea of this work is to prepare sustainable ACs from local resources by direct and physical activation using steam.

Two agricultural residues were selected: sugar beet pulp, a typical French waste accounting for 33 million tons per year, and peanut hulls, a Mexican waste with an annual production of 70,000 tons. As for arsenic contamination of surface and ground water, this is a worldwide problem due to its established toxicity and its presence in overcrowded areas.[2] In 1993, the guideline concentration limit in drinking water recommended by the WHO was fixed at 10 μg. L^{-1}. The European Union has accepted this value in their regulatory systems but in Mexico, for example, it is still 25 $\mu g.L^{-1}$.[3]

Two predominant species found in natural waters are inorganic forms of arsenic, namely arsenate, As (V), and arsenite, As (III), and their presence depends on the pH and redox conditions. As (V) is the thermodynamically stable form, found in oxic surface waters, rivers and lakes, and presents three pKa: 2.2, 7 and 11.6. This means that in most natural waters, arsenic (V) is mainly in the $H_2AsO_4^-$ form (at $3 < pH < 6$) or associated with the $HAsO_4^{2-}$ form (at $6.5 < pH < 7.5$). Above pH 8, $HAsO_4^{2-}$ is the predominant species.[4] Although various technologies are well known for the removal of arsenic from waters, adsorption is one of the best available to achieve the lowest concentration in the effluent after treatment.[5]

The most widely studied media for adsorption processes include iron hydroxide and oxide, such as amorphous

Address correspondence to Claire Gerente, LUNAM Université, Ecole des Mines de Nante, CNRS, GEPEA, UMR 6144, 4 rue Alfred Kastler, BP 20722, 44307, Nantes cedex 03, France; E-mail: claire.gerente@mines-nantes.fr

Table 1. Selection of papers reporting the adsorption of arsenic onto activated carbons.

Steam-activated carbons from agricultural residues				
Precursor	*Activation conditions*	*q_m of As (III) $\mu g\ g^{-1}$*	*q_m of As (V) $\mu g\ g^{-1}$*	*Ref.*
Oat hulls	H_2O, Fast pyrolysis (500°C, 1.5 s).	—	3100	[12]
Olive pulp	H_2O, 800°C, 2 h.	1390	—	[13]
Bean pod waste	H_2O, 700°C, 1h.	1010	—	[14]
Commercial activated carbons modified with iron				
	Impregnation conditions	*Iron content%*	*q_m of As (V) $\mu g\ g^{-1}$*	*Ref.*
NC100	0.05 M $FeCl_3$ solution in acidic media for 6 hours.	2.2	28	[15]
NC100	0.05 M $FeCl_3$ solution in acidic media for 24 hours.	9.4	8	[15]
Lignite-based GC	Iron impregnation with Fe (III).	7.0	4500	[16]
Commercial (UltraCarb)	By evaporation of $Fe(NO_3)_3{\cdot}9H_2O$ solution at pH 6, no Fe precipitation was observed.	11.7	51,300	[17]
Commercial (UltraCarb)	By evaporation of $Fe(NO)_3{\cdot}9H_2O$ solution at pH 8, no Fe precipitation was observed.	11.17	43,600	[17]
Commercial granular (Super Darco)	0.5–1 g mL^{-1} [$Fe(NO_3)_3{\cdot}9H_2O$] solution dispersed on carbon followed by evaporation for Fe oxide/hydroxide precipitation.	7.5–11	4000–19000	[18]
Commercial granular	2.5% Fe^{+3} ferric chloride solution at pH 12.	4.8	25	[19]
Commercial (NC100)	0.05 M $FeCl_3$ and 3 M HCl solution.	0.5–0.75	25–30	[20]
Commercial (NC100)	0.05 M $FeCl_3$ and 0.5 M HCl solution.	1.3–1.5	15–20	[20]

hydrous ferric oxide, ferrihydrite and goethite, activated alumina, zeolites and chitosan.[6–11] As far as activated carbons are concerned, only a few recent publications have shown that physical activation of agricultural residues by steam leads to carbonaceous materials which are effective for As removal.[12–14] On the other hand, in the last decade more than 10 papers have reported that arsenic sorption capacities are enhanced when ACs are impregnated with iron salt solutions, with or without a preliminary oxidation step.[15–20]

The combination of activated carbon and iron loading is attractive: AC is as an ideal support medium for iron preloading due to its high BET surface area while iron has a high affinity for arsenate and arsenite. However, all these modifications have only been conducted on commercial materials. Table 1 reports a selection of these papers and focuses on (i) physically activated carbons prepared from agricultural residues and (ii) commercial activated carbons modified with iron for arsenic removal. Regarding arsenate removal, only one study[12] describes activated carbons obtained from steam activation of oat hulls with a maximum capacity, deduced from the Langmuir model, of 3100 $\mu g.g^{-1}$. As far as commercial activated carbons are concerned, different impregnations are possible leading to an iron content ranging between 2.2 and 11.7% and q_m values for arsenate are very scattered from 0.008 to 51.3 $\mu g.g^{-1}$.[15, 17]

This work thus has two main objectives. First, the conversion of cheap and renewable agricultural residues into sustainable ACs is studied in a one-step process with steam activation. The second aim is to show the value of these ACs for As (V) removal, including the improved and tailored AC after iron impregnation. After a physical and chemical characterization of the porous materials, adsorption experiments are performed in terms of contact time experiments, adsorption isotherms in deionized and natural waters and the effect of a preliminary oxidation. Different models are presented: intraparticle diffusion and pseudo–second-order equations for kinetic data, and Langmuir and Freundlich models for equilibrium data.

Materials and methods

All chemicals were of reagent grade from Sigma. Arsenic solutions were made from Na_2HAsO_4-$7H_2O$. Sugar beet pulp was commercially supplied by Lyven (Cagny, France) and peanut hulls were obtained from a local market. In a previous study, a complete characterization of the raw sugar beet pulp revealed that polysaccharides accounted for 72.5% of the dry matter, ash for 3.9% and calcium for 1.1%.[21] Raw peanut hulls had an ash content of 1.7%. In addition, a commercial granular activated carbon (GAC), also produced from a biomass (coconut) and physically activated with steam, was used as a reference for the physicochemical characterization and for comparison of sorption performances.

Activated carbon production

The sugar beet pulp (BP) and peanut hulls (PH) were first dried at 110°C for 24 hours before being heated at 10°C

min^{-1} up to 850°C under a nitrogen flow rate of 0.5 L min^{-1}. At 850°C, steam was also introduced into the furnace at 0.7 mL min^{-1} for 80 min. Then, heating was stopped and the fall in temperature occurred while still under the nitrogen atmosphere. These conditions were optimized from a previous study,[22] and they are resolutely placed in the field of sustainable production because (i) only local resources are investigated, (ii) direct activation is used and (iii) no chemicals are employed as activating agents.

The activated carbonaceous materials thus obtained from beet pulp and peanut hulls were called BP-H_2O and PH-H_2O, respectively. Next, they were crushed in a hammer mill and the particles were sieved so that only particle sizes of 0.50–1.00 mm were used for the arsenic adsorption experiments. This fraction was washed with deionized water (10 g L^{-1}) until the pH remained constant, filtered and dried at 110°C. Mass yields were 16 and 24% for BP-H_2O and PH-H_2O, respectively. To obtain iron-modified ACs, 1 g of BP-H_2O and PH-H_2O were also placed in a $FeCl_3$-$6H_2O$ solution (0.1 M and pH = 1.7) and the mixture was shaken for 24 hours at room temperature.

Once again, this modification is in agreement with sustainable development since no toxic chemicals are used (only $FeCl_3$-$6H_2O$), with no added oxidant and no additional heating.[15–20] Iron-impregnated beet pulp activated carbon (BP-H_2O-Fe) and iron-impregnated peanut hull carbon (PH-H_2O-Fe) were then washed several times with deionized water until water was free of iron. The iron content of BP-H_2O-Fe and PH-H_2O-Fe was measured after an acid digestion (concentrated HCl), by an atomic absorption spectrophotometer with flame atomization (AAS Analyst 400, Perkin Elmer). Finally, the adsorbents were dried at 105°C.

Activated carbon characterization

Physical characterization – BET surface area analysis

Textural parameters of the samples, like surface area and porosity, were obtained from nitrogen adsorption isotherms. In order to eliminate any adsorbed humidity and/or gases, between 0.8–1.2 g of the carbon was outgassed at 350°C for 24 hours. Then, N_2 isotherms were recorded at 77 K using automatic equipment (ASAP 2010, Micromeritics). The total pore volume (V_{total}) and specific surface area (S_{BET}) of the adsorbents were obtained from the Brunauer-Emmet-Teller (BET) isotherm model.

In addition, Horvath-Kawazoe (HK) and Barret, Joyner and Halenda (BJH) models were used to evaluate the micropore (V_{micro}) and mesopore (V_{meso}) volumes. The micropores have diameters of less than 2 nm while the mesopores have diameters between 2 and 50 nm. All the results were duplicated but the raw materials (sugar beet pulp and peanut hulls) were not characterized due to their poor specific surface areas and absence of porosity. The entire study was carried out with the same precursors and no adsorption of As (V) onto the raw materials was observed.

Elemental analysis and total ash content

Each sample was ground into a fine powder for the determination of elemental content (Flash EA 1112, Thermofinnigan). This analysis was repeated three times for each sample to provide an average reading. Results were indicated as percentages of carbon, hydrogen, nitrogen and oxygen. No sulfur content was detected. The total ash content in percentage was calculated by the standard test method for activated carbon.[23]

pH_{PZC} determination

This was carried out as follows: 100 mL of 0.1 M NaCl solution was placed in a closed Erlenmeyer flask and the pH was adjusted to between 2 and 12 by adding solutions of HCl or NaOH (0.1 M). Then, 0.05 g of each sample was added and the final pH measured after 5 days under stirring at room temperature. The pH_{PZC} is the point where the curve pH_{final} vs. $pH_{initial}$ crosses the line $pH_{final} = pH_{initial}$.[24]

EDX and SEM

The porous structure of the carbonaceous materials and commercial activated carbons was observed using a JEOL 6400F Scanning Electron Microscope. A magnification ranging from 100X to 500X was used for visualization of the images. Imaging is typically achieved using secondary electrons to obtain the best resolution of the fine surface typographical features. An EDX analysis was carried out to verify the presence of iron on the surface of the modified carbons.

Arsenic removal with AC

Sorption kinetic experiments

Batch contact time experiments were conducted at 20°C by stirring 0.05 g of adsorbent with 100 mL of As (V) solution (1000 μg L^{-1}), at 200 rpm. Initial pH values were close to 6 and were recorded at the end of the experiment. For each adsorbent, the equilibrium time between the solid and the solution was determined by plotting C_t versus time.

To investigate the mechanism of sorption, two kinetic models were tested. The intraparticle diffusion-controlled adsorption model is generally applied to porous powdered materials and at the beginning of the kinetic decay curve in order to determine the intraparticle diffusion rate constant.[25] Eq. 1 expresses the adsorption capacity as a function of time, where k_i is the intraparticle diffusion rate constant (mg g^{-1} $min^{-0.5}$):

$$q_t = k_i t^{0.5} \quad (1)$$

The adsorbents were thus ground into powder and new kinetic curves were carried out during the first 2 hours of the decay, with vigorous stirring (300 rpm) at 20°C. The k_i values for each material were deduced from the slope of the line q_t versus $t^{0.5}$.

The second model is the pseudo–second-order sorption model proposed by Ho and McKay[26] and used to describe the whole kinetic decay curve. Its equation is the following (Eq. 2)

$$dq_t/dt = k_2(q_e - q_t)^2 \quad (2)$$

where q_t (μg g^{-1}) is the amount of arsenate in the material at any time t (min), q_e (μg g^{-1}) is the amount of arsenate sorbed at equilibrium and k_2 (g μg^{-1} min^{-1}) is the rate constant of the pseudo–second-order equation. Taking into account the boundary condition $q_t = 0$ at $t = 0$, and the initial sorption rate h (μg g^{-1} min^{-1}),

$$h = k_2 q_e^2 \quad (3)$$

Eq. 2 can be rearranged to obtain:

$$t/q_t = 1/h + 1/q_e t \quad (4)$$

By plotting t/q_t versus t, the values of h, k_2, q_e calculated were determined for all the materials.

Adsorption isotherms

Batch adsorption isotherms were conducted with 100 mL of synthetic solutions from 100 to 5000 μg L^{-1} of arsenate and 0.05 g of activated carbons. The bottles were sealed and put on a shaker for 5 days at 20°C. After shaking, the equilibrium pH was measured and recorded, the samples were filtered through a 0.45-μm regenerated cellulose filter and the concentration of arsenic in the filtrate was determined by atomic absorption spectroscopy with a graphite tube (AAS Analyst 600, Perkin Elmer). Analytical measurements were obtained with a quantification limit of 4 μg L^{-1} and a detection limit of 2 μg L^{-1}. It was verified when necessary that no adsorption occurred on the walls of the plastic bottles or on the filters. Langmuir and Freundlich models were applied to describe the experimental results. The Langmuir equation[27] is the following (Equation 5):

$$q_e = \frac{bq_m C_e}{1 + bC_e} \quad (5)$$

where q_e (μg g^{-1}) and C_e (μg L^{-1}) are the amount of arsenic at equilibrium in the solid and liquid phase, respectively. q_m and b are the parameters representing the maximum sorption capacity (μg g^{-1}) and the sorption constant (L μg^{-1}), respectively. According to the Langmuir model assumptions, adsorption occurs in a monolayer coverage characterized by the q_m value, on homogeneous adsorption sites of constant energy, and adsorbed species do not interact with each other. The empirical Freundlich model[28] is formulated as:

$$q_e = K_f C_e^n \quad (6)$$

K_f ($\mu g^{1-1/n}$ $L^{1/n}$ g^{-1}) and n are the Freundlich constants that indicate the adsorption capacity and the heterogeneity factor, respectively. The assumptions are (i) the adsorption sites of different energy are heterogeneous; (ii) the adsorbed species could interact with each other; and, (iii) there is no upper limit to adsorption, which restricts its use to diluted media.

In adsorption processes, it is well known that the presence of other ions in solution can greatly modify the sorption capacities. To determine this effect, sorption isotherms were also conducted in two natural spring waters, called HMC and LMC for high mineral content water and low mineral content water respectively, whose compositions are shown in Table 2. The main differences are in their anion concentrations, especially SO_4^{2-}, HCO_3^- and Cl^-, which can potentially lead to competition with arsenate species and, to a lesser extent, the cation content like Ca^{2+}, Mg^{2+} and Na^+. These spring waters were spiked with arsenic from 100 to 5000 μg L^{-1} and the same protocol was followed for the adsorption isotherms.

Results and discussion

Characterization of the activated carbons

Before the sorption experiments, the four activated carbons produced at lab scale from sugar beet pulp (BP-H_2O and BP-H_2O-Fe) and peanut hulls (PH-H_2O and PH-H_2O-Fe) were characterized in terms of their textural properties (BET surface area, porous volumes, micro/mesoporosity percentage), chemical composition (elemental analysis, ash content, pH_{PZC}) and SEM pictures. GAC was used as a reference.

Table 2. Mineral content of spring waters used for As (V) adsorption.

Water	Ca^{2+}	Mg^{2+}	Na^+	K^+	Cl^-	NO_3^-	HCO_3^-	SO_4^{2-}	*pH*
HMC (mg.L^{-1})*	230	66	40	8	58	< 1	280	620	7.2
LMC (mg.L^{-1})**	4.1	1.7	2.7	0.9	0.9	0.8	25.8	1.1	7.3

*Spring water with a high mineral content (HMC), **Spring water with a low mineral content (LMC).

Table 3. Characterization of activated carbons produced from sugar beet pulp, peanut hulls and commercial GAC.

	BP-H_2O	*BP-H_2O-Fe*	*PH-H_2O*	*PH-H_2O-Fe*	*GAC*
S_{BET} (m^2 g^{-1})	821	762	829	718	1138
V_{micro} (cm^3 g^{-1})	0.3478	0.3227	0.3551	0.3084	0.4852
V_{meso} (cm^3 g^{-1})	0.3612	0.3227	0.0699	0.0569	0.1761
Microporosity%	49	50	84	84	73
Mesoporosity%	51	50	16	16	27
Total porous volume (cm^3 g^{-1})	0.6430	0.5778	0.4028	0.3446	0.6230
C%	77.9	67.8	91.2	83.9	90.1
H%	0.9	1.0	0.8	0.6	0.2
N%	0.6	0.7	0.2	0.4	ns
O%	7	16	6	14	9
Fe%	0.1	4.8	ns	0.5	ns
Ash%	13.6	13.9	1.3	1.5	0.4
pH_{PZC}	9.8	9	9.8	6	8

ns: not significant.

Physical characterization – BET surface area analysis

The results provided by nitrogen adsorption isotherms are presented in Table 3. The BET surface areas are 821 and 762 m^2 g^{-1} for BP-H_2O and BP-H_2O-Fe, and 829 and 718 m^2 g^{-1} for PH-H_2O and PH-H_2O-Fe, respectively. Previously, determinations of BET surface area were done on a char (without activation) from sugar beet pulp and on the raw precursor (data not shown) but the results revealed very low values of 6.6 m^2 g^{-1} and 0.2 m^2 g^{-1}, respectively.[21] These values confirm that activation is necessary to create porosity in a carbonaceous material.

Another point to note is that the iron impregnation on BP-H_2O and PH-H_2O only causes a slight reduction in the BET surface area, leading to 762 m^2 g^{-1} for BP-H_2O-Fe and 718 m^2 g^{-1} for PH-H_2O-Fe. Although the precipitation of iron is difficult to control because of the complexity and black color of the mixture, it can be deduced that iron impregnation is probably not a homogeneous coating that closes the porosity but rather an amount of iron oxide probably fixed in specific sites. The SEM pictures and EDX spectra confirm this assumption (Fig. 1). The BET surface areas developed by BP-H_2O and PH-H_2O are 25% lower than for GAC.

Taking into account that our first goal was not the optimization of the AC production, in terms of activation temperature, nature of activating gas, temperature ramp and dwell time, these values are considered acceptable for activated carbons produced at laboratory scale. To demonstrate this, a selection of papers is reported in Table 4 based on agricultural residues, the conditions of physical activation, BET surface areas and total porous volumes of the obtained ACs.[29–34] It is clear that the BET surface area depends on the precursor, the nature of the activating gas and the activation temperature.

In a study by El-Hendawy et al.,[29] the corncob was first carbonized at 500°C for 2 hours and a portion of this char was steam-activated at different temperatures (from 600°C to 850°C) and times (1 to 2 hours). The resulting BET surface areas ranged between 607 and 786 m^2 g^{-1}. In another case, an increase of 90°C in activation temperature induced an enhancement of BET surface area from 446 to 607 m^2 g^{-1} on an AC produced from bagasse.[31] On the other hand, CO_2 activation led to the highest BET surface areas in the same range of temperatures.[32] Nevertheless, in all cases, the BET surface areas determined in this work, from sugar beet pulp and peanut hulls, are quite high in comparison with the data from this literature review.

Considering the experimental total porous volumes, the value obtained with sugar beet pulp (BP-H_2O) is similar to those of GAC: 0.643 cm^3 g^{-1} compared to 0.623 cm^3 g^{-1}, respectively, while PH-H_2O presents a lower volume of 0.403 cm^3 g^{-1}. Once again, iron impregnation causes little effect on the porous volumes (−10% in BP-H_2O and −14% in PH-H_2O). They are also greatly improved in comparison with the values shown in Table 3. Looking at the balance between microporous and mesoporous volumes, PH-H_2O is the highest microporous carbon (84%), followed by GAC (73%) and then BP-H_2O (50%).

However, BP-H_2O and PH-H_2O have similar microporous volumes (0.35 cm^3 g^{-1}). As far as iron-modified activated carbons are concerned, impregnation does not modify the percentage in terms of micro- and mesoporosity. In the composition of raw sugar beet pulp, a high percentage of ash was observed (4%) corresponding to the natural presence of calcium ions.[21] Consequently, the ash content of the carbon obtained is also high at 14% (Table 3). More generally, high ash content in the precursor tends to decrease the microporous volume balance. This observation has already been made in a previous work where activated carbons produced from raw bagasse with a high ash content (15%) by physical activation had some inorganic oxides filling or blocking a part of the microporous volume.[34]

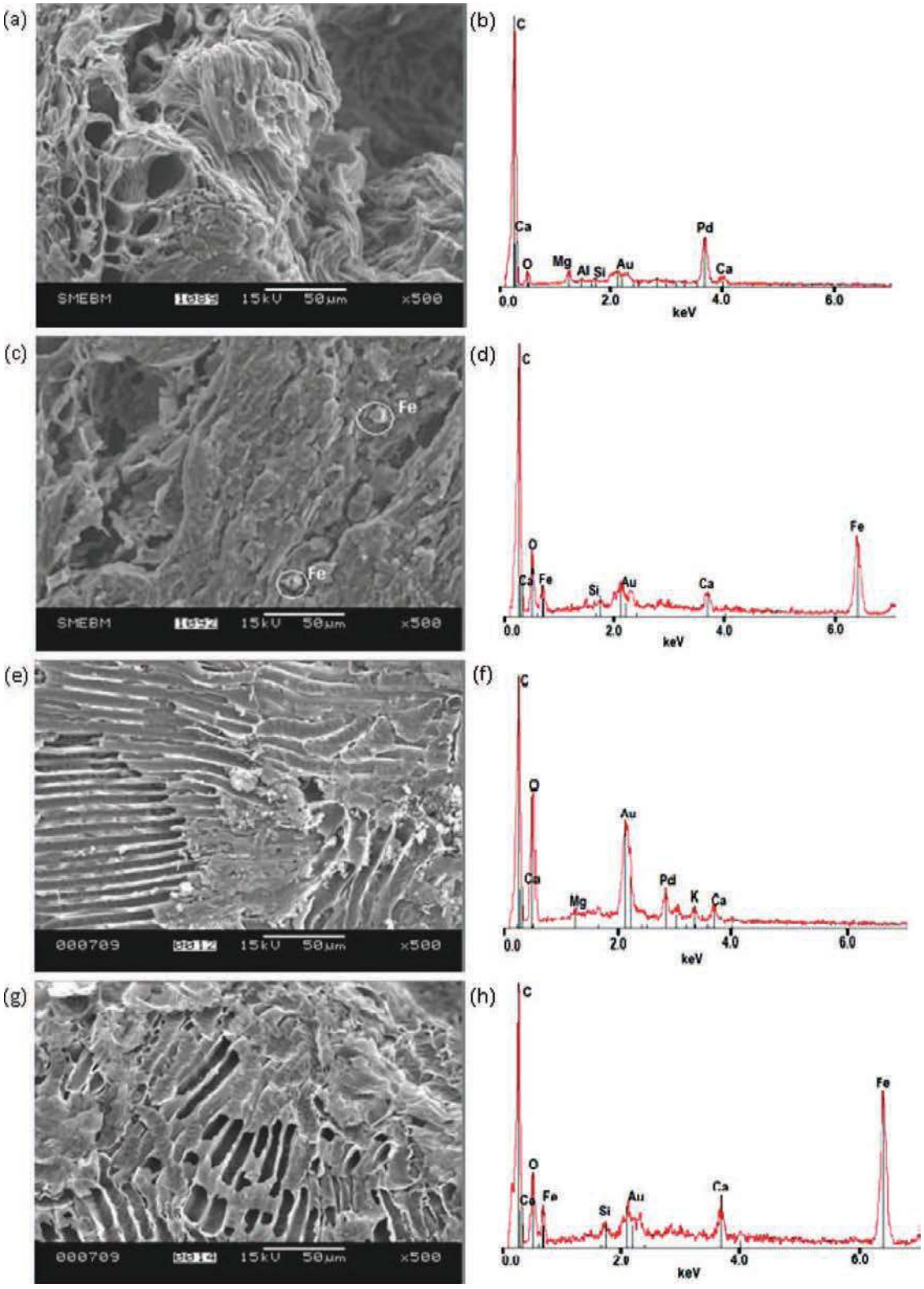

Fig. 1. SEM micrographs and EDX spectra of BP-H_2O (a-b), BP-H_2O-Fe (c-d), PH-H_2O (e-f), PH-H_2O-Fe (g-h) (color figure available online).

Table 4. Selection of papers dealing with the production of activated carbons from agricultural residues, in similar conditions to this work.

Material	*Activation conditions*	S_{BET} ($m^2\ g^{-1}$)	*Total porous volume* ($cm^3\ g^{-1}$)	*Reference*
Corncob	Steam/850°C (1 h)	607	0.296	[29]
	Steam/600°C (2 h)	618	0.321	
	Steam/700°C (2 h)	786	0.430	
Sawdust	Steam/800°C (1 h)	516	–	[30]
Bagasse	Steam/750°C (2 h)	446	0.287	[31]
	Steam/840 °C (2 h)	607	0.445	
Pistachio nut-shells	CO_2/800°C(1 h)	884	–	[32]
	CO_2/800°C(2.5 h)	964		
Macadamia nut-shells	CO_2/500°C(4 h)	750	–	[33]
Bagasse	CO_2/900°C(1 h)	614	0.310	[34]
Beet pulp	Steam/850°C(1.3 h)	821	0.643	This work
Peanut hulls	Steam/850°C(1.3 h)	829	0.403	This work

Another study using activated sludge with more than 20% ash as the precursor led to the same result.[35]

Chemical characterization: Elemental analysis and pH_{PZC}

The major element contents, C, H, N and O, are given in Table 3. The carbon percentage is 78% and 68% for BP-H_2O and BP-H_2O-Fe and 91% and 84% for PH-H_2O and PH-H_2O-Fe, respectively. These values depend on the precursor but are still comparable to the carbon content of a commercial GAC (90%). In that sense, the adsorbents produced from sugar beet pulp and peanut hulls are really activated carbons, with a high carbon content. The second major element is oxygen. Although the determination by elemental analysis is sometimes tricky, it gives an order of magnitude confirmed by triplicates.

BP-H_2O, PH-H_2O and GAC present similar percentages (7%, 6% and 9%, respectively) and these increase in both BP-H_2O-Fe and PH-H_2O-Fe after iron impregnation (16% and 14%, respectively). It should be noted that the $FeCl_3$ solution has an acidic pH of 1.7, which probably favored some surface oxidation of the sorbents and consequently the oxygen content. In BP-H_2O-Fe and PH-H_2O-Fe, the iron concentration was determined after an acid digestion of the sorbents and measured by atomic absorption spectrometry. The iron content deduced from this methodology is 4.8 and 0.5% for BP-H_2O-Fe and PH-H_2O-Fe, respectively.

The efficiency of this impregnation method depends on the nature of the precursor but leads to an increase in iron content compared with BP-H_2O (0.1%) and PH-H_2O (not significant). From the state of the art process (Table 1), modified commercial ACs can exhibit higher iron concentrations because the methodologies employed are often either preceded by an oxidation step or followed by solution evaporation or thermal treatment.

A methodology adapted from Faria et al.[24] and based on pH measurement was used to determine the pH of point of zero charge (pH_{PZC}). It depends on the chemical and electronic properties of the functional groups on the surface and so is a good indicator of these properties. After an optimized contact time of 5 days, if the final pH of the solution is the same as before the AC introduction, then this is the pH_{PZC}.

Moreover, it is generally admitted that (i) at pH $<$ pH_{PZC}, the overall surface charge of the solid is mostly protonated thus positively charged, (ii) at pH = pH_{PZC}, the surface presents an equal positive and negative charge, and (iii) at pH $>$ pH_{PZC}, the overall surface charge of the solid is mostly deprotonated thus negatively charged.[36] BP-H_2O, BP-H_2O-Fe, PH-H_2O and GAC reveal strong basic behavior with pH_{PZC} ranging from 8 to 9.8 (Table 3).

This means that when placed in solution, they will induce a basic pH, which is useful because it gives an idea of the pH variation during the sorption experiments. After iron impregnation, it has been shown that O content increases after a partial oxidation of the surface. However, it probably also leads to an increase in the oxygenated chemical moieties like carboxyl, lactone, lactol or hydroxyl groups. Thus, pH_{PZC} decreases from 9.8 to 9 for BP-H_2O and BP-H_2O-Fe and from 9.8 to 6 for PH-H_2O and PH-H_2O-Fe. The latter acidic value is surprising and needs to be confirmed by further experiments on surface chemical moieties.

Scanning electron microscopy (SEM)

Surface images of the carbonaceous materials were analyzed by scanning electron microscopy as shown in Figure 1 (a, c, e and g). From these pictures, it is possible to appreciate the rough edges of the surface of the materials. Only Figure 1(c) (BP-H_2O-Fe) shows clearly the presence of iron

traces and just in specific spots on the surface. To complete these pictures, EDX spectra were carried out on BP-H_2O, BP-H_2O-Fe, PH-H_2O and PH-H_2O-Fe (Fig. 1(b, d, f and h)). These were only used for a qualitative analysis: carbon and oxygen are the major elements present in all samples, no iron is observed on BP-H_2O and PH-H_2O, and its content in BP-H_2O-Fe is higher than in PH-H_2O-Fe because of the size of the peak which was confirmed in the previous section.

Arsenic removal with carbonaceous materials and GAC

Sorption kinetics

Batch contact experiments were conducted on BP-H_2O, BP-H_2O-Fe, PH-H_2O, PH-H_2O-Fe and GAC and the kinetic decay curves are plotted in Figures 2a and 2b. It has previously been verified that no adsorption occurs on raw beet pulp and the corresponding char (data not shown) so

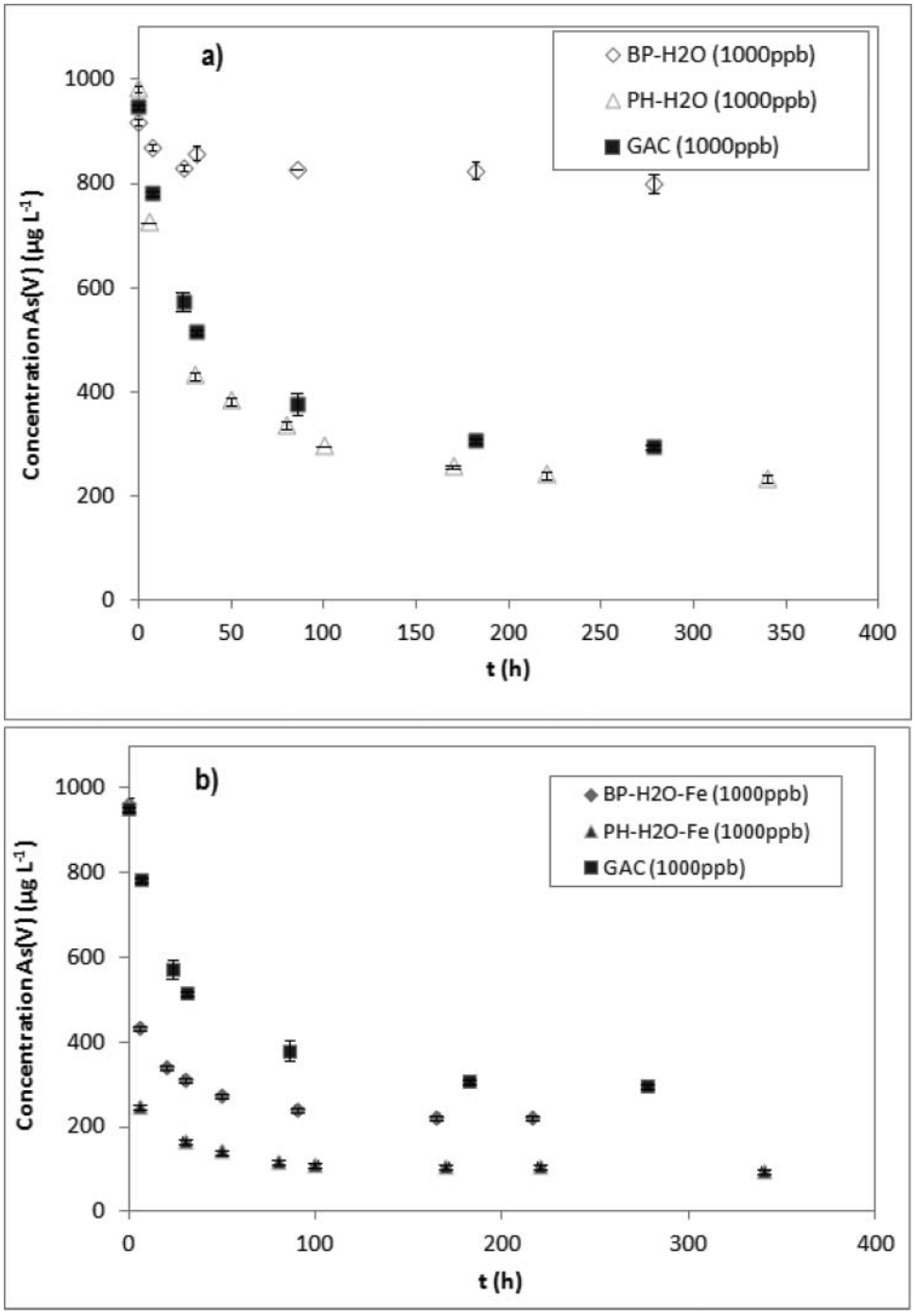

Fig. 2. Kinetic decay curves for removal of As (V) on (a) BP-H_2O, PH-H_2O and GAC and (b) BP H_2O-Fe, PH-H_2O-Fe and GAC.

Table 5. Parameters of intraparticle diffusion and pseudo–second-order kinetic models.

	Intraparticle diffusion		*Pseudo–second-order*				
Material	k_{id} ($\mu g\ g^{-1}\ min^{-0.5}$)	R^2	h ($\mu g\ g^{-1}\ min^{-1}$)	$q_{e,\ calc.}$ ($\mu g\ g^{-1}$)	$q_{e,\ exp}$ ($\mu g\ g^{-1}$)	k_2 ($g\ \mu g^{-1}\ min^{-1}$)	R^2
BP-H_2O	31	0.939	0.50	188.7	194.5	1.42×10^{-5}	0.990
BP-H_2O-Fe	84	0.947	7.06	833.3	853.8	1.02×10^{-5}	1.000
PH-H_2O	24	0.983	1.91	909.1	875.6	2.31×10^{-6}	0.999
PH-H_2O-Fe	88	0.959	14.27	909.1	928.4	1.73×10^{-5}	1.000
GAC	41	0.988	1.42	833.3	832.5	2.04×10^{-6}	0.996

that activation is essential for arsenate adsorption. The optimal contact time deduced from the curves and common to all the materials is 120 h (5 days). The comparison of kinetic data obtained with BP-H_2O, PH-H_2O and GAC (Fig. 2a) shows that PH-H_2O and GAC have a similar behavior in terms of rate and uptake amounts. After iron impregnation (Fig. 2b), the capacities are undoubtedly enhanced and kinetic rates seem to be faster. As this chemical treatment slightly affects the porous structure, a chemisorption reaction is probably involved.

To investigate the mechanism of sorption and potential rate-controlling steps, kinetic models were used to describe the experimental data. The intraparticle diffusion-controlled adsorption model (Eq. 1) requires the adsorbent to be reduced to powder and focuses on the first hours of the kinetic curves.[25] If the rate-limiting step is intraparticle diffusion, a plot of the sorbed solute against the square root of contact time should yield a straight line passing through the origin.[37] The model led to acceptable correlation coefficients (Table 5) suggesting that intraparticle diffusion is probably a limiting step of the adsorption reaction between activated carbons and arsenate ions. The results also show that BP-H_2O-Fe and PH-H_2O-Fe exhibit higher intraparticle diffusion constants. As diffusivity is a function of the solute affinity for the adsorbent material and the activated carbon site density, it can be confirmed that As (V) has a great affinity for iron-loaded sorbents.[38]

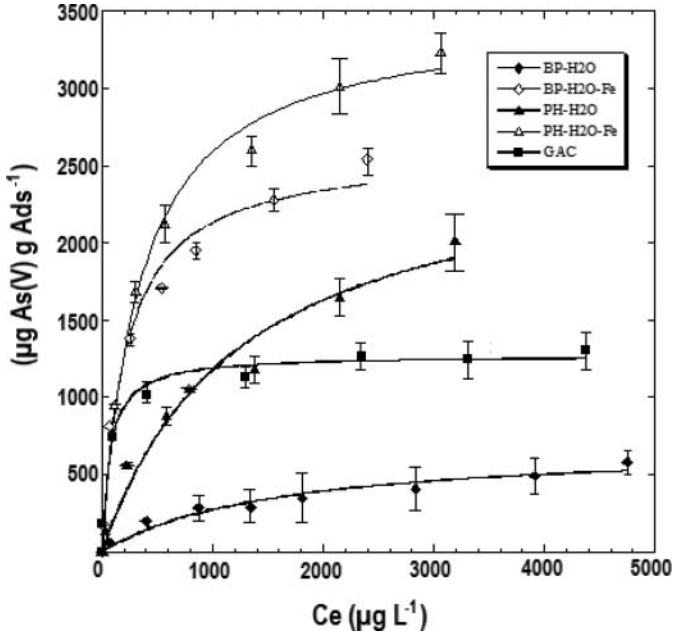

Fig. 3. Experimental adsorption isotherms of As (V) and modeled results using the Langmuir equation.

The pseudo–second-order model[26] (Equations 2–4) was also tested and it described the experimental data perfectly: as shown in Table 5, the R^2 values are close to unity and the calculated q_e values are similar to the experimental ones, demonstrating that the pseudo–second-order model can be applied to the whole curve. This is also in agreement with a chemisorption mechanism being the rate-controlling step. Nevertheless, it is a pseudo-kinetic model, so a specific but different rate constant is obtained for each change in a system variable.

However, all the curves are obtained in the same experimental conditions and the constants are compared with each other. It is clear from Table 5 that iron impregnation increases the initial sorption rate (h) by a factor of 14 on BP-H_2O-Fe (7.06 $\mu g\ g^{-1}\ min^{-1}$) and by a factor of 7 on PH-H_2O-Fe (14.27 $\mu g\ g^{-1}\ min^{-1}$). Moreover, the h values obtained with PH-H_2O and GAC are similar, 1.91 and 1.42 $\mu g\ g^{-1}\ min^{-1}$ respectively, and higher than BP-H_2O (0.5 $\mu g\ g^{-1}\ min^{-1}$). In another work, kinetic data on arsenic sorption from groundwater (initial concentration of 300 $\mu g\ L^{-1}$) using commercial iron-doped activated carbons were also presented.[15] Initial sorption rates deduced from the pseudo–second-order model were of the same order of magnitude, ranging between 0.65 and 38.1 $\mu g\ g^{-1}\ min^{-1}$.

Adsorption isotherms

Adsorption isotherms were conducted with 120 h of contact time between the arsenate solution (initial concentrations ranged between 100 to 5000 $\mu g\ L^{-1}$ and pH between 6 and 7) and ACs. Experimental points, as well as the curves modeled by Langmuir and Freundlich equations, are shown in Figures 3 and 4. The constants of each model are reported in Table 6.

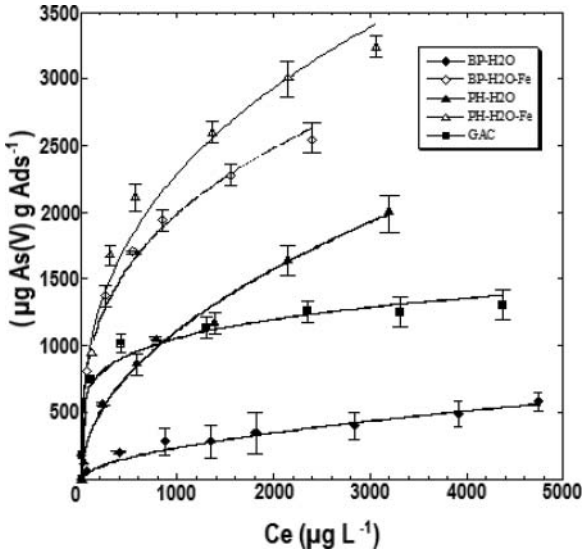

Fig. 4. Experimental adsorption isotherms of As (V) and modeled results using the Freundlich equation.

Based on the determination factor (Table 6), the experimental data fit the Freundlich model ($R^2 = 0.968$–0.993) better than the Langmuir model ($R^2 = 0.956$–0.971) for the carbonaceous materials. The maximum capacities deduced from the Langmuir model are 690 and 2820 μg g^{-1} for steam-activated materials (BP-H_2O and PH-H_2O), 2930 and 3280 μg g^{-1} for iron-modified carbons (BP-H_2O-Fe and PH-H_2O-Fe) and 1240 μg g^{-1} for GAC. These values calculated from the model are similar to the experimental ones. It is also clear that iron impregnation greatly improves the uptake of arsenate.

Regarding the Freundlich model, K_F values are found to be 5 and 30 $\mu g^{1-1/n}$ $L^{1/n}$ g^{-1} for steam-activated carbons (BP-H_2O and PH-H_2O), 205 and 640 $\mu g^{1-1/n}$ $L^{1/n}$ g^{-1}for iron-loaded materials and 300 $\mu g^{1-1/n}$ $L^{1/n}$ g^{-1} for GAC. The values for n are less than 1 in all cases, which indicates that adsorption is favorable.[39] The pH at the end of the isotherm depends on the AC. It is higher than initial values (6 to 7) for BP-H_2O and BP-H_2O-Fe (9 to 9.5 and 8.5 to 9, respectively), similar for PH-H_2O and GAC (6.5 to 7) and lower for PH-H_2O-Fe (4.5 to 6).

This means that the main arsenate species present in solution is $H_2AsO_4^-$ and that this is also the main species adsorbed on PH-H_2O-Fe, PH-H_2O and GAC. On the contrary, $HAsO_4^{2-}$ is probably the form sorbed on BP-H_2O and BP-H_2O-Fe. In these conditions, all the sorbents are rather protonated because all the final pH values are below the pH_{PZC}.

Thus, positively-charged surfaces could react favorably with the negative species of arsenate. Iron impregnation involves a combination of two effects: first, it strongly increases the initial adsorption rates and uptake capacities of both BP-H_2O-Fe and PH-H_2O-Fe, confirming the great affinity between arsenate ions and iron-based sorbents. Secondly, and to a lesser extent, it decreases the pH_{PZC} and subsequently the solution pH. This leads to the monovalent ion ($H_2AsO_4^-$) being the major arsenate species present whose adsorption is the highest on PH-H_2O-Fe exhibiting only 0.5% of iron.

Finally, the results of many studies (Table 1) have shown the advantages of commercial iron-impregnated AC but have also revealed large discrepancies between the q_m values (from 20 μg g^{-1} to more than 50 000 μg g^{-1}). Nevertheless, the latter seem to be correlated with the iron content. The results obtained in this work are correctly placed within this field if we consider activated carbons produced from agricultural wastes at laboratory scale thus trying to increase the iron content of the proposed sorbent should be an interesting perspective.

To show the potential effect of competing ions, adsorption isotherms were conducted in natural waters (Fig. 5a and 5b) whose major components are shown in Table 2 and to which arsenic was added. PH-H_2O and PH-H_2O-Fe, the best activated carbons in terms of adsorption capacities, were selected for this experiment. From Figure 5b, it is clear that in high mineral content water, PH-H_2O loses its adsorptive properties completely. On the contrary, isotherms carried out with PH-H_2O-Fe on both natural waters (Fig. 5a) exhibit weakened but useful capacities compared to GAC. The isotherm curves clearly show some waves that prevented the Langmuir or Freundlich models from being tested. Iron impregnation seems to moderate the competitive effect of anion or cationic, monovalent or divalent ions and is necessary for the adsorbents to keep their capacities in natural waters.

Table 6. Adsorption constants for Langmuir and Freundlich models.

	Langmuir			*Freundlich*		
Material	q_m ($\mu g\ g^{-1}$)	b_L ($L\ \mu g^{-1}$)	R^2	K_F ($\mu g^{1-1/n}\ L^{1/n}\ g^{-1}$)	n	R^2
BP-H_2O	690	0.00066	0.956	5	0.56	0.968
BP-H_2O-Fe	2930	0.00312	0.964	205	0.33	0.990
PH-H_2O	2820	0.00066	0.971	30	0.52	0.993
PH-H_2O-Fe	3280	0.00089	0.945	640	0.21	0.991
GAC	1240	0.01454	0.966	300	0.18	0.968

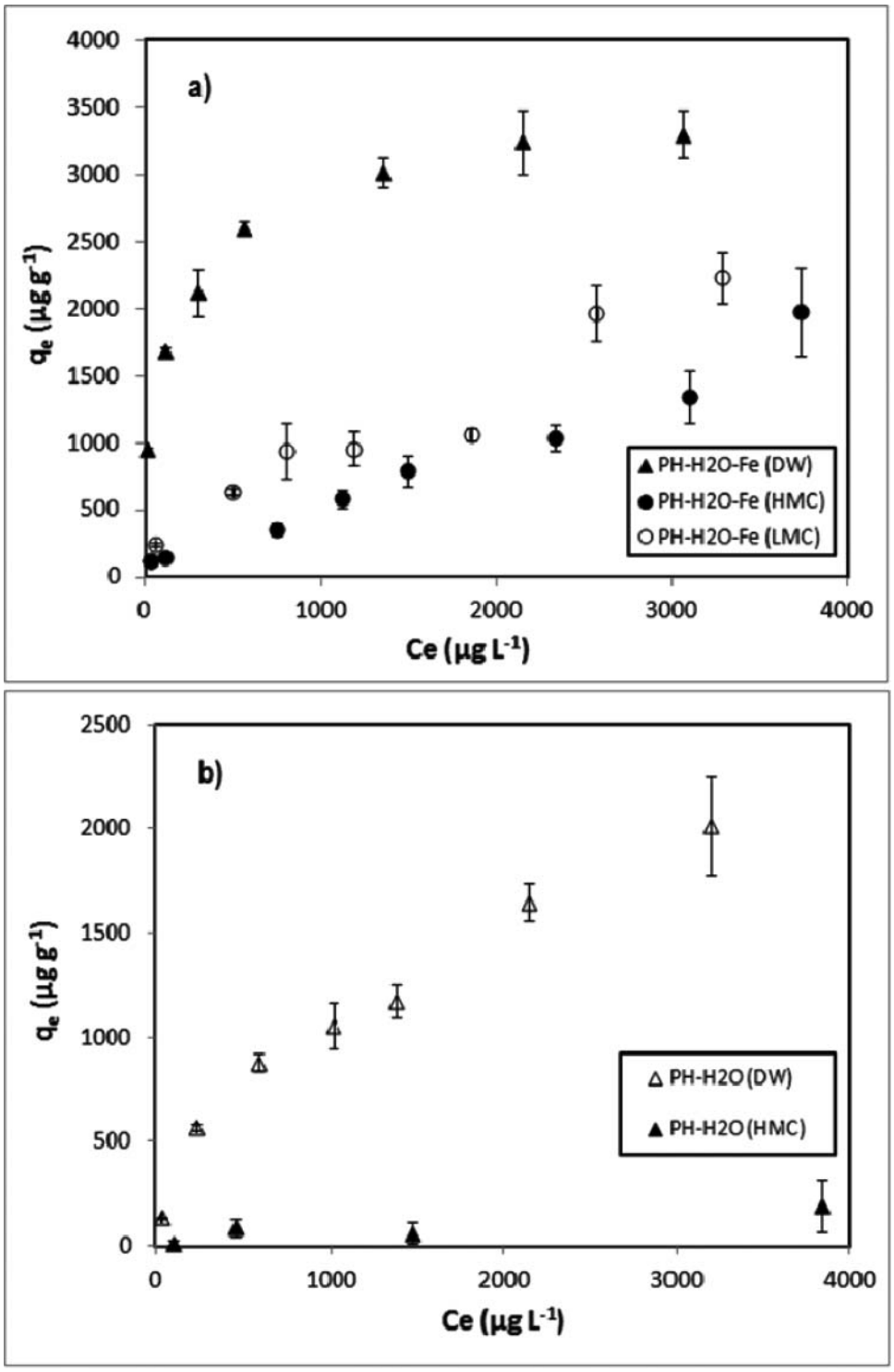

Fig. 5. Sorption isotherm of arsenic (V) onto: (a) PH-H_2O-Fe and (b) PH-H_2O in deionized water (DW) and spring water with a high (HMC) or low (LMC) mineral content.

Conclusions

The aim of this work was to prepare sustainable activated carbons from agricultural wastes, namely sugar beet pulp and peanut hulls, and to use them to remove arsenate from water. A direct physical activation by steam led to activated carbons, called BP-H_2O and PH-H_2O, with respective mass yields of 16% and 24%. A chemical treatment by iron impregnation was performed leading to 4.8% and 0.5% of iron in BP-H_2O and PH-H_2O. An investigation of the porous structure showed that the BET surface area is close to 800 $m^2\ g^{-1}$ for both adsorbents, total porous volume is higher in BP-H_2O (0.64 $cm^3\ g^{-1}$) than in PH-H_2O (0.40 $cm^3\ g^{-1}$) but microporous volumes are similar (0.35 $cm^3\ g^{-1}$).

Moreover, BP-H_2O-Fe and PH-H_2O-Fe keep their porous properties after iron impregnation. Carbon contents are up to 70% and ash contents depend greatly on the precursor. pH_{PZC} measurements reveal a clear basic behavior, except for PH-H_2O-Fe. Based on these results, the production of activated carbons from agricultural residues is clearly successful at lab scale. In terms of arsenic removal, the carbonaceous sorbents need first to be steam-activated and then iron-impregnated to increase adsorption capacities. From kinetic studies, the equilibrium time is close to 120 hours and the rate-controlling steps are probably related to intraparticle diffusion and chemisorption.

Regarding equilibrium data, experimental isotherms are correctly described by the Langmuir and Freundlich models. The best fit is obtained with the Freundlich equation while the best q_m values provided by Langmuir are 3280 $\mu g\ g^{-1}$ for PH-H_2O-Fe, 2930 $\mu g\ g^{-1}$ for BP-H_2O-Fe, 2820 $\mu g\ g^{-1}$ for PH-H_2O and 690 $\mu g\ g^{-1}$ for BP-H_2O. In natural waters, the results also confirm the good performances of iron-rich materials. Iron impregnation creates a double effect: first, it strongly increases the initial adsorption rates and uptake capacities for both BP-H_2O-Fe and PH-H_2O-Fe. Secondly, it decreases the pH_{PZC} of the adsorbents and subsequently the solution pH leading to a majority of the adsorbable arsenate species $H_2AsO_4^-$. This study displays that sustainable AC produced at laboratory scale, improved by a simple chemical treatment and successfully applied to arsenate removal, could be used in a continuous process.

Acknowledgments

We acknowledge financial support from the Consejo Nacional de Ciencia y Tecnología de México (CONACYT) by a scholarship grant for JTP.

References

[1] Ioannidou, O.; Zabaniotou, A. Agricultural residues as precursors for activated carbon production - a review. Renew. Sust. Energ. Rev. **2007**, *11*, 1966–2005.

[2] Jain, C.K.; Ali, I. Arsenic: occurrence, toxicity and speciation techniques. Wat. Res. **2000**, *34*, 4304–4312.

[3] NOM. Salud ambiental. Agua para uso y consumo humano. Límites permisibles de calidad y tratamientos a que debe someterse el agua para su potabilización. Norma Oficial Mexicana **2000**, NOM-127-SSA1-1994 (in Spanish).

[4] Sengupta, A.K.; Greenleaf, J.E. Arsenic in subsurface water: Its chemistry and removal by engineered processes. In *Environmental separation of heavy metals. Engineering Processes*; Lewis Publishers Eds; Boca Ratón, USA, **2002**; 160–215.

[5] Mohan, D.; Pittman, C.U. Arsenic removal from water/wastewater using adsorbents - a critical review. J. Hazard. Mat. **2007**, *142*, 1–53.

[6] Raven, K.P.; Jain, A.; Loeppert, R.H. Arsenite and arsenate adsorption on ferrihydrite: kinetics, equilibrium, and adsorption envelope. Environ. Sci. Technol. **1998**, *32*, 344–349.

[7] Driehaus, W.; Jekel, M.; Hiildebrandt, U. Granular ferric hydroxide - a new adsorbent for the removal of arsenic from natural water. J. Water SRT Aqua **1998**, *47*, 30–35.

[8] Appelo, C.; Weiden, V.; Tournassat, C.; Charlet, L. Surface complexation of ferrous iron and carbonate on ferrihydrite and the mobilization of arsenic. Environ. Sci. Technol. **2002**, *36*, 3096–3103.

[9] Singh, T.S.; Pant, K.K. Equilibrium, kinetic and thermodynamic studies for adsorption of As(III) on activated alumina. Separ. Purif. Technol. **2004**, *36*, 139–147.

[10] Jimenez-Cedillo, M.J.; Olguin, M.T.; Fall, C. Adsorption kinetic of arsenates as water pollutant on iron, manganese and iron-manganese-modified clinoptilolite-rich tuffs. J. Hazard. Mat. **2009**,*163*, 939–945.

[11] Gerente, C.; McKay, G.; Andrès, Y.; Le Cloirec, P. Interactions of natural aminated polymers with different species of arsenic at low concentrations: Application in water treatment adsorption. Adsorption **2005**, *11*, 859–863.

[12] Chuang, C.L.; Fan, M.; Xu, M.; Brown, R.C.; Sung, S.; Saha, B.; Huang, C.P. Adsorption of arsenic(V) by activated carbon prepared from oat hulls. Chemosphere **2005**, *61*, 478–483.

[13] Budinova, T.; Petrov, N.; Razvigorova, M.; Parra, J.; Galiatsatou, P. Removal of arsenic(III) from aqueous solution by activated carbons prepared from solvent extracted olive pulp and olive stones. Ind. Eng. Chem. Res. **2006**, *45*, 1896–1901.

[14] Budinova, T.; Savova, D.; Tsyntsarski, B.; Ania, C.O.; Cabal, B.; Parra, J.B.; Petrov, N. Biomass waste-derived activated carbon from the removal of arsenic and manganese ions from aqueous solutions. Appl. Surf. Chem. **2009**, *255*, 4650–4657.

[15] Fierro, V.; Muñiz, G.; Gonzalez-Sánchez, G.; Ballinas, M.L.; Celzard, A. Arsenic removal by iron-doped activated carbons prepared by ferric chloride forced hydrolysis. J. Hazard. Mat. **2009**, *168*, 430–437.

[16] Reed, B.; Vaughan, R.; Jiang, L. As(III), As(V), Hg and Pb removal by Fe-oxide impregnated activated carbon. J. Env. Eng. **2000**, *126*, 869–873.

[17] Chen, W.; Parette, R.; Zou, J.; Cannon, F.S.; Dempsey, B.A. Arsenic removal by iron-modified activated carbon. Water Res. **2007**, *41*, 1851–1858.

[18] Jang, M.; Chen, W.F.; Cannon, F.S. Preloading hydrous ferric oxide into granular activated carbon for arsenic removal. Environ. Sci. Technol. **2008**, *42*, 3369–3374.

[19] Mondal, P.; Majumder, C.B.; Mohanty, B. Effects of adsorbent dose, its particle size and initial arsenic concentration on the removal of arsenic, iron and manganese from simulated ground water by Fe^{3+} impregnated activated carbon. J. Hazard. Mater. **2008**, *150*, 695–702.

[20] Muñiz, G.; Fierro, V.; Celzard, A.; Furdin, G.; Gonzalez-Sánchez, G.; Ballinas, M.L. Synthesis, characterization and performance in arsenic removal of iron-doped activated carbons prepared by impregnation with Fe(III) and Fe(II). J. Hazard. Mater. **2009**, *165*, 893–902.

[21] Reddad, Z.; Gerente, C.; Andrès, Y.; Ralet, M.C.; Thibault, J.; Le Cloirec, P. Ni(II) and Cu(II) binding properties of native and modified sugar beet pulp. Carbohydr. Polym. **2002**, *49*, 23–31.

[22] Rio, S.; Le Coq, L.; Faur, C.; Lecomte, D.; Le Cloirec, P. Preparation of adsorbents from sewage sludge by steam activation for industrial emission treatment. Process Safety and Environmental Protection **2006**, *B4*, 258–264.

[23] ASTM Standards. Standard Test Method for Total Ash content of Activated Carbon. Ann. Book Amer. Soc. Test. Mater. **1994**, *15*, 478.

[24] Faria, P.C.C.; Orfao, J.J.M.; Pereira, M.F.R. Adsorption of anionic and cationic dyes on activated carbons with different surface chemistries. Water Res. **2004**, *38*, 2043–2052.

[25] Morris, J.C.; Weber, W.J. Removal of biologically-resistant pollutants from waste waters by adsorption - Advances in Water Pollutions Research, In 1st Conf. Was. Pollut. Res. Proceedings, Pergamon Press, New York, **1962** (2): 231–266.

[26] Ho, Y.S.; McKay, G. Kinetic models for the sorption of dye from aqueous solution by wood. Trans. IchemE. **1998**, *76*, 183–191.

[27] Langmuir, I. The constitution and fundamental properties of solids and liquids. J. Amer. Chem. Soc. **1916**, *38*, 2221–2295.

[28] Freundlich, H.M. Over the adsorption in solution. J. Phys. Chem. **1906**, *57*, 385–470.

[29] El-Hendawy, A.N.A.; Samra, S.E.; Girgis, B.S. Adsorption characteristics of activated carbons obtained from corncobs. Coll. and Surf. A: Physicochemical and Engineering Aspects **2001**, *180*, 209–221.

[30] Malik, P.K. Use of activated carbons prepared from sawdust and rice-husk for adsorption of acid dyes: a case study of Acid Yellow 36. Dyes Pigments **2003**, *56*, 239–249.

[31] Juang, R.S.; Wu, F.C.; Tseng, R.L. Characterization and use of activated carbons prepared from bagasses for liquid-phase adsorption. Coll. Surf. A: Physicochem. Eng. Aspects **2002**, *201*, 191–199.

[32] Yang, T.; Lua, A.C. Characteristics of activated carbons prepared from pistachio-nut shells by physical activation. J Coll. Interf. Sci. **2003**, *267*, 408–417.

[33] Wang, Z.M.; Kanoh, H.; Kaneko, K.; Lu, G.O.; Do, D. Structural and surface property changes of macadamia nut-shell char upon activation and high temperature treatment. Carbon **2002**, *40*, 1231–1239.

[34] Valix, M.; Cheung, W.H.; McKay, G. Preparation of activated carbon using low temperature carbonization and physical activation of high ash raw bagasse for acid dye adsorption. Chemosphere **2004**, *56*, 493–501.

[35] Julcour Lebigue, C.; Andriantsiferana, C.; Krou, N.; Ayral, C.; Mohameda, E.; Wilhelm, A-M.; Delmas, H.; Le Coq, L.; Gerente, C.; Smith, K.M.; Pullket, S.; Fowler, G.D.; Graham, N.J.D. Application of sludge-based carbonaceous materials in an hybrid water treatment process based on adsorption and catalytic wet air oxidation. J. Environ. Man. **2010**, *91*, 2432–2439.

[36] Rivera-Utrilla, J.; Bautista-Toledo, I.; Ferro-Garcia, M.A.; Moreno-Castilla, C. Activated carbon surface modification by adsorption of bacteria and their effect on aqueous lead adsorption. J. Chem. Technol. Biotechnol. **2001**, *76*, 1206–1216.

[37] Gérente, C.; Lee, V.K.C.; LeCloirec, P.; McKay, G. Application of chitosan for the removal of metals from wastewaters by adsorption - Mechanisms and models review. Crit. Rev. Environ. Sci. Technol. **2007**, *37*, 41–127.

[38] Axe, L.; Trivedi, P. Intraparticle surface diffusion of metal contaminants and their attenuation in microporous amorphous Al, Fe, and Mn oxides. J. Coll. Interf. Sci. **2002**, *247*, 259–265.

[39] LeVan, M.D.; Carta, G.; Yon, C.M. Adsorption and ion exchange. In *Perry's Chemical Engineers Handbook*; McGraw-Hill, New York, **1997**; Vol. 16, 11.